Materials Chemistry and Physics 162 (2015) 364–371

Contents lists available at ScienceDirect

Materials Chemistry and Physics

journal homepage: www.elsevier.com/locate/matchemphys

Thermostability and photophysical properties of mixed-ligand carboxylate/benzimidazole Zn(II)-coordination polymers

Bráulio Silva Barros [a, *], Jaroslaw Chojnacki [b], Antonia Alice Macêdo Soares [c], Joanna Kulesza [c], Leonis Lourenço da Luz [c], Severino Alves Júnior [c]

[a] School of Science and Technology, Federal University of Rio Grande do Norte (UFRN), Campus Universitário Lagoa Nova, 59078-970 Natal, RN, Brazil
[b] Department of Inorganic Chemistry, Chemical Faculty, Gdansk University of Technology, G. Narutowicza 11/12, 80-233 Gdansk, Poland
[c] Department of Fundamental Chemistry, Federal University of Pernambuco (UFPE), Av. Prof. Moraes Rego, 1235 – Cidade Universitária, 50670-901 Recife, PE, Brazil

HIGHLIGHTS

- Structurally different Zn(II)-coordination polymers were prepared.
- The formation of frameworks was counter anion and temperature dependent.
- Photoluminescence in the wide range of the spectrum, from UV to IR was observed.
- Thermostability and luminescence depended on bzim packing in the structure.

GRAPHICAL ABSTRACT

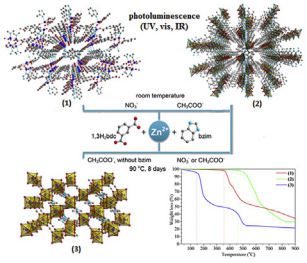

ARTICLE INFO

Article history:
Received 27 March 2015
Received in revised form
14 May 2015
Accepted 30 May 2015
Available online 9 June 2015

Keywords:
Microporous materials
Crystal structure
Photoluminescence spectroscopy
Thermal properties

ABSTRACT

The reaction between $Zn(NO_3)_2 \cdot 6H_2O$ or $Zn(CH_3COO)_2 \cdot 2H_2O$ and isophthalic acid (1,3-H_2bdc) in the presence of benzimidazole (Hbzim) in dimethylformamide (DMF)/ethanol (EtOH)/H_2O solvent mixture at room temperature yielded two structurally different coordination polymers: $[Zn_2(1,3\text{-bdc})_2(Hbzim)_2]$ **(1)** and $[Zn_2(1,3\text{-bdc})(bzim)_2]$ **(2)**. **(1)** is a 2D-layered framework with a molecule of benzimidazole coordinated to the Zn center, whereas **(2)** is a 3D framework with benzimidazolate species acting as a co-ligand and bridging two Zn(II) ions. Reactions performed at 90 °C led to the formation of coordination polymers structurally similar to **(2)**, independently of the Zn(II) source used. In the absence of benzimidazole, the reaction between $ZnAc_2.2H_2O$ and 1,3-H_2bdc at 90 °C resulted in the formation of **(3)**, a 3D coordination polymer $Zn(HCOO)_3(Me_2NH_2^+)$. It was observed that the thermostability and the photophysical properties of **(1)** and **(2)** are strongly dependent on the coordination modes and packing of benzimidazole in the solid state. These materials present photoluminescence in the wide range of the spectrum, from UV to IR. A full understanding of a physical process occurring in these intriguing systems, including complete energy level diagrams with possible transitions were provided.

1. Introduction

In the last decade, coordination polymers and metal-organic frameworks have received considerable attention and their synthesis and properties are constantly reviewed, to cite only the

* Corresponding author.
E-mail address: brauliobarros@ect.ufrn.br (B.S. Barros).

http://dx.doi.org/10.1016/j.matchemphys.2015.05.079
0254-0584/

recent reports [1–5]. These materials exhibit intriguing structures, interesting topologies and potential applications in gas storage, sensing and separation [6–8], catalysis [9], drug delivery [10], etc. Luminescent coordination polymers are of particular interest and posses several advantages over other luminescent materials. The structural diversity, well-defined orientation of organic linkers in the lattice and the possibility of permanent porosity with host–-guest interactions promote interesting and unique luminescent properties in these materials. Coordination polymers based on d^{10} metal centers such as Zn(II) or Cd(II) and π-conjugated organic ligands have been investigated because of their tunable fluorescent properties and potential application as photoactive materials, especially those with high thermal stability [11–15]. As the Zn^{2+} or Cd^{2+} ions are difficult to oxidize or reduced due to their closed-shell d^{10} configuration, their luminescent properties are originated mainly from the organic ligand (intraligand fluorescent emission) although ligand-to-metal charge transfer transitions have been also observed [16,17].

In the solid state organic rigid linkers are closely-packed due to the π–π interactions of aromatic rings. The control of ligand-to-ligand interactions and ligand-to-metal coordination modes permits to obtain tunable fluorescent properties. From this point of view, the systematic studies on structure–property relationship are still crucial in this field.

Considerable efforts have been done to understand the factors that govern the formation and final structure of coordination polymers. Whereas the coordination geometry of the metal center, ligand and solvent properties are the parameters that in a relatively comprehensible way affect the final structure, the role of a counter ion on the formation of supramolecular architectures is not always clear [18–20]. Counter ions are often included in charged frameworks to preserve the charge balance by coordination to the metal cluster or by accommodation into the pores and/or channels [21,22]. Moreover, counter ions affect the crystallization of products leading to different frameworks [23,24]. Therefore, their properties, such as size, charge, shape, coordination ability, ability to form hydrogen bonds or other weak interactions, may direct the final structure.

Several reports on Zn(II)-coordination polymers with isophthalate and substituted benzimidazoles, often so-called flexible *N*-bridging ligands with two linked benzimidazole residues can be found in the literature and their luminescent properties have been investigated [25–31]. Nevertheless, deeper studies on the photophysical processes occurring in these systems, including the investigation of the possible transitions also in the IR region have never been undertaken.

In the present work, three structurally different Zn^{2+}-coordination polymers based on carboxylate and/or benzimidazole ligands were prepared depending on the type of the counter ion and the temperature used in the synthesis. The thermal and photophysical properties of the two obtained Zn(II) mixed-ligand coordination polymers differed by the linkers packing in the solid state were studied and compared, and the structure–properties relationship was investigated. The energy diagrams with possible transitions occurring in both coordination polymers and for comparison, in the free ligands, were constructed. According to our best knowledge, such profound photophysical studies have never been reported before.

2. Experimental section

2.1. Materials and methods

All reagents and solvents were used as received without further purification. Isophthalic acid (1,3-H_2bdc) and benzimidazole (Hbzim) were purchased from Sigma Aldrich. $Zn(NO_3)_2{\cdot}6H_2O$, $Zn(CH_3COO)_2{\cdot}2H_2O$ ($ZnAc_2{\cdot}2H_2O$) and solvents: dimethylformamide (DMF) and ethanol (EtOH) were purchased from Vetec. Single-crystal X-ray diffraction data were collected on a KUMA KM4CCD κ-axis diffractometer with graphite monochromated Mo Kα radiation (λ = 0.71073 Å) at 120 K. Powder X-ray diffraction (PXRD) data were recorded at room temperature on a Bruker D8 Advance diffractometer with Cu Kα (λ = 1.5406 Å) radiation. Thermogravimetric analyzes (TGA) were performed on a Shimadzu DTG-60H thermal analysis system. Samples were heated from 30 °C to 900 °C at a rate of 20 °C/min under nitrogen atmosphere. Fourier Transform Infrared spectra (FT-IR) were measured on a Bruker spectrometer (model IFS66) at the range of 4000–700 cm^{-1} using KBr pellets. Absorption peaks were described as follows: very strong (vs), strong (s), medium (m) and weak (w). The photoluminescent properties of the ligands (1,3-H_2bdc and Hbzim) and of the obtained coordination polymers were collected in the solid state at room temperature using a FLUOROLOG3 ISA/Jobin-Yvon spectrofluorometer equipped with Hamamatsu R928P photomultiplier, SPEX 1934 D phosphorimeter and a pulsed 150 W Xe–Hg lamp.

2.2. Preparation of Zn(II)-coordination polymers

It was found that the type of counter anion (acetate or nitrate) in the synthesis between Zn^{2+} salt and isophthalic acid in the presence of benzimidazole play a crucial role in the self-assembly process, yielding structurally different coordination polymers. Such phenomenon was observed only at room temperature, whereas at 90 °C always the same framework was obtained, independently of the Zn(II) source used (see details in Supporting Information). In the absence of benzimidazole, the reaction performed at 90 °C led to the formation of Zn-formate framework, as a consequence of the hydrolysis of the solvent DMF [32].

Zn_2(1,3-bdc)$_2$(Hbzim)$_2$ **(1)** was prepared as follows: 1 mmol (0.166 g) of isophthalic acid and 0.5 mmol (0.06 g) of benzimidazole were dissolved in 10 mL of DMF/EtOH mixture (5/5 mL) and stirred for 10 min to assure the complete dissolution of reactants. Subsequently, an aqueous solution (5 mL) of $Zn(NO_3)_2{\cdot}6H_2O$ (0.298 g, 1 mmol) was added. The mixture was left standing at room temperature for six months. The resulting colorless crystals of **(1)** suitable for X-ray analysis, were filtered off, washed with DMF and water and dried in an oven at 60 °C for 2 h. Yield: 30.2% based on Zn. Selected IR peaks (KBr pellet, υ/cm^{-1}): 1625 (s), 1606 (s), 1572 (s), 1434 (m), 1398 (s), 1362 (s), 1323 (s), 1306 (s), 1273 (m), 1260 (m), 1250 (m), 736 (vs), 718 (vs). Anal. Calcd for Zn_2(1,3-bdc)$_2$(bzim)$_2$: C, 51.85; H 2.88; N, 8.06%. Found: C, 51.45; H 2.78; N 8.15%.

Zn_2(1,3-bdc)(bzim)$_2$ **(2)** was obtained within similar to **(1)** synthetic conditions except that $Zn(CH_3COO)_2{\cdot}2H_2O$ (0.220 g, 1 mmol) was used instead of $Zn(NO_3)_2{\cdot}6H_2O$. The white powder of **(2)** was obtained after two weeks. Yield: 41.6% based on Zn. Selected IR peaks (KBr pellet, υ/cm^{-1}): 1601 (m), 1534 (s), 1479 (m), 1453 (s), 1405 (s), 1296 (m), 1275 (m), 1241 (s), 1198 (w), 1183 (w), 912 (m), 843 (w), 778 (m), 734 (vs). Anal. Calcd for Zn_2(1,3-bdc)(bzim)$_2$: C, 49.90; H 2.65; N, 10.59%. Found: C, 49.16; H 1.26; N 10.48%.

$Zn(HCOO)_3(Me_2NH_2^+)$ **(3)** resulted from the reaction of isophthalic acid and $Zn(CH_3COO)_2{\cdot}2H_2O$ performed at 90 °C for 8 days in the absence of benzimidazole. The subsequent slow solvent evaporation at room temperature for six months led to the colorless cubic crystals of **(3)** suitable for X-ray analysis. Yield: 30.2% based on Zn. Selected IR peaks (KBr pellet, υ/cm^{-1}): 3000 (w), 1569 (vs), 1471 (w), 1458 (w), 1439 (w), 1343 (vs), 1027 (w), 796 (vs). Anal. Calcd for $Zn(HCOO)_3(Me_2NH_2^+)$: C, 24.35; H 4.46; N, 5.68%. Found: C, 24.25; H 4.35; N 5.60%.

2.3. X-ray Crystallography

The collected data were processed using the CrysAlisPro (Agilent Technologies) program package [33]. Empirical absorption correction (multi-scan) was applied using spherical harmonics, implemented in SCALE3 ABSPACK scaling algorithm of the CrysAlisPro package. An initial structure model was obtained by charge flipping (SUPERFLIP, Palatinus) [34]. Calculations were carried out using the SHELX system [35] run under WINGX environment [36]. Hydrogen atoms were refined as riding on carbon atoms or for the N–H atoms refined as independent, only with the interatomic distances constrained to 0.85 Å.

3. Results and discussion

3.1. Structures description

The structure of the framework **(1)** is reported here for the first time. Crystal data for **(1)** are summarized in Table 1. Selected bond distances and hydrogen-bond geometry for compound **(1)** are listed in Tables S1 and S2 (see Supplementary Information).

Coordination polymer **(1)** crystallizes in the triclinic system in the space group $P\bar{1}$. Asymmetric unit (Fig. 1) contains two zinc ions bound to two terminal benzimidazole ligands and two bridging isophthalate anions (μ-1,3-bdc). Both zinc atoms are five-coordinated by one nitrogen atom and four oxygen atoms. Zn1 is chelated (η_2) by O5 (more distant) and O6 (closer) from one carboxylic group, and forms two η_1 bonds with O1 and O8 from different anions. Zn2 cannot be regarded as chelated by its neighbor carboxylic anion with O3 and O4, since Zn2–O3 distance is much longer than Zn2–O4 bond (2.654 and 2.024 Å, respectively). Apart of that Zn2 is bound to O7 and O2 from different anions and additionally links with O6 atom from the COO^- group, which chelates Zn1 atom. Thus, O6 bridges the two metal atoms. Covalent and coordination bonds span the entire crystal forming a 2D coordination polymer. The layer has no internal symmetry and as such belongs to the *p*1 (L1) type of subperiodic layer groups [37] with **a'** = **a** and **b'** = **b**.

The backbone forms a 2D framework with (4, 4) topology.

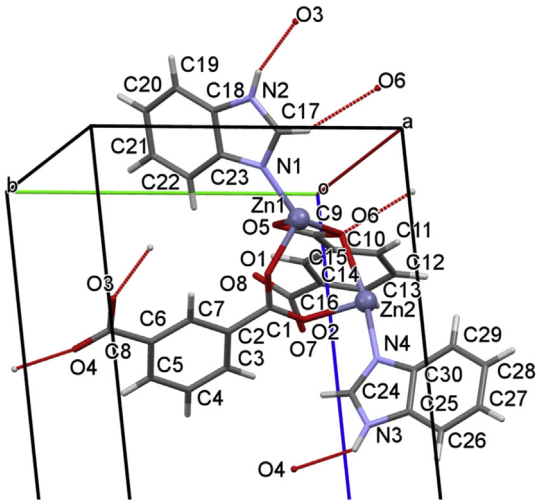

Fig. 1. Asymmetric unit of (1) with atom labeling scheme. Zinc atoms shown as balls; hydrogen atoms not labeled. Color code: dark gray-carbon, light gray-hydrogen, red-oxygen, light blue-nitrogen, dark blue-zinc. Red dashed lines present intermolecular hydrogen bonds. (For interpretation of the references to colour in this figure legend, the reader is referred to the web version of this article.)

Separation of Zn1 and Zn2 in the asymmetric unit, 3.309 Å, is much smaller than any other Zn...Zn distances, the next shortest being: 8.255 Å Zn1 ...$Zn2^{\#1}$ (#1 = x, 1 + y, z), and then Zn1...Zn1 or Zn2...Zn2 = 9.364 Å = *a* (basis axis). Each node of the web contains two zinc atoms with two benzimidazole ligands, and the spacers are isophthalate anions which link the nodes into the tetragonal grid (Fig. 2) extending parallel to the plane (001). Packing of the layers in the crystal is reinforced by the formation of hydrogen bonds of the NH...O type between the grids (see Fig. 1 and Table S2 of Supporting Information). Additional C17–H···O6 (charge assisted) bonds also operate among the substructures. The layers are "separable" and no interpenetration was found. No larger voids could be detected in the structure. So, the structure is composed of covalently bound 2D layers which are assembled into a supramolecular 3D structure by hydrogen bonding.

The structure of obtained framework **(2)** shown in Fig. 3, has already been reported in the literature by Cui et al. [38]. In this structure, the benzimidazole species are included in the structure and act as a bridge between two zinc ions. Therefore, the Zn atom in an approximately tetrahedral geometry is coordinated by two

Table 1
Crystallographic data for **(1)**.

	(1)
Empirical formula	$C_{30}H_{20}N_4O_8Zn_2$
Formula weight	695.24
Crystal size (mm)	0.27 × 0.12 × 0.08 mm
Crystal system	Triclinic
Space group	$P\bar{1}$
a (Å)	9.3640 (4)
b (Å)	10.0220 (4)
c (Å)	14.5735 (7)
α (°)	88.255 (4)
β (°)	77.797 (4)
γ (°)	88.269 (4)
V (Å^3)	1335.75 (10)
Z	2
λ (Å)	0.71073
d_{calc} (g cm^{-3})	1.729
T(K)	120
μ (mm^{-1})	1.86
F(000)	704
h, k, l max	11, 12, 17
N_{ref}	4972
θ_{min}, θ_{max} (°)	2.5, 25.5
R_1 (I > 2σ(I))	0.046
wR_2(I > 2σ(I))	0.132

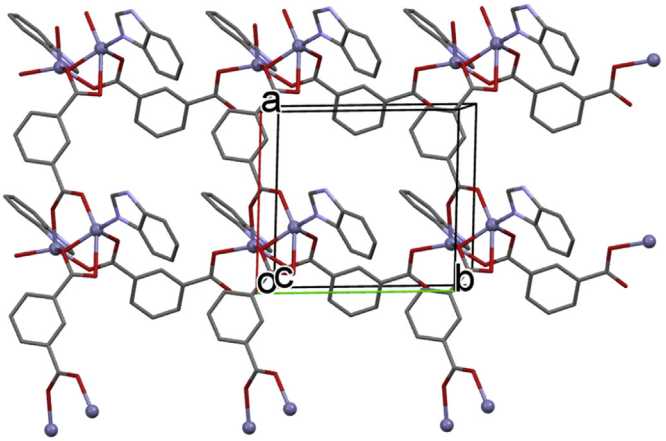

Fig. 2. View of (1) along the c axis, presenting the 2D grid in the coordination polymer.

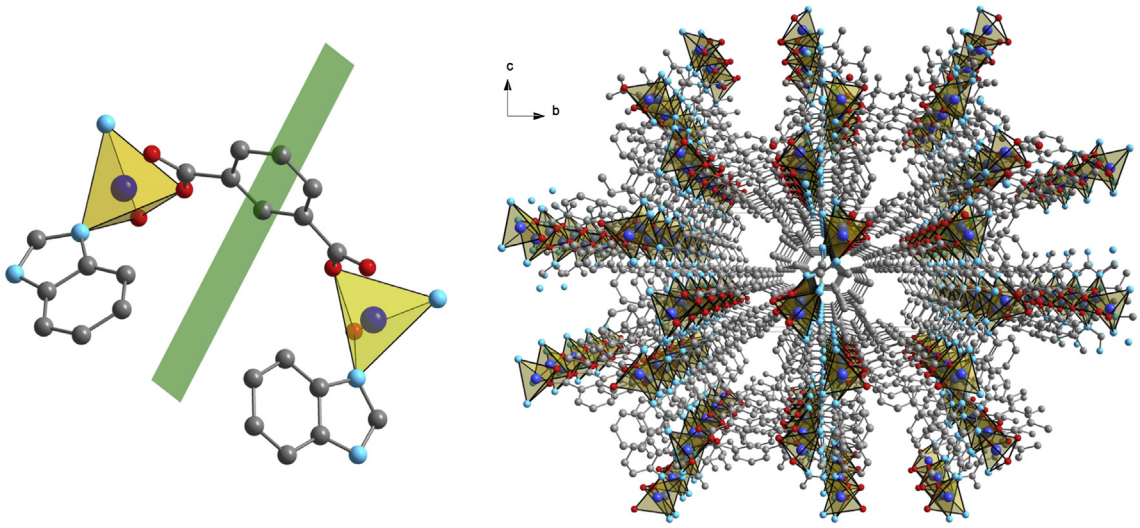

Fig. 3. Asymmetric unit combined with its plane reflection – shown in green (on the left) and projection along the a axis (on the right) of the partially expanded net structure of (2). Zinc centers shown as yellow tetrahedra, hydrogen not shown. Color code: gray-carbon, red-oxygen, light blue-nitrogen, dark blue-zinc. (For interpretation of the references to colour in this figure legend, the reader is referred to the web version of this article.)

nitrogen atoms of two different benzimidazolate ligands and two oxygen atoms coming from two different 1,3-bdc ligands. Each carboxylate groups adopt bidentate *syn-anti* bridging coordination mode.

The crystal structure of **(3)** consists of a 3D metal-organic framework with perovskite-like architecture constructed by Zn^{2+} cations linked by deprotonated formate anions ($HCOO^-$). The dimethyl ammonium cations $(CH_3)_2NH_2^+$ are located in the pores of the structure. Such structure has already been reported in the literature [39–41]. Since the quality of the new phase solution is similar to those already reported, it has not been deposited it at CCDC.

The coordination environment around Zn^{2+} cations is slightly distorted octahedral formed by six oxygen atoms of formate linkers. Each carboxylate is coordinated to the zinc center via the bi(monodentate) bridging mode. Fig. 4 presents the structure of **(3)** with accommodated (disordered) $(CH_3)_2NH_2^+$ cations within the channels.

3.2. Sample characterization

The PXRD patterns of obtained samples **(1–3)** and the simulated PXRD patterns of the polymers (**2**) and (**3**) calculated from single crystal data available in the literature [38,41] are shown in Fig. 5. The PXRD patterns of coordination polymers **(2)** and **(3)** match well with the corresponding simulated patterns of $[Zn_2(1,3\text{-bdc})(bzim)_2]$ and $(Me_2NH_2^+)[Zn(HCOO)_3]$, respectively, confirming the formation of pure-phase structurally similar frameworks. In the case of **(3)**, the differences in the relative intensity of the diffraction peaks in comparison with the simulated XRD pattern, are noticed. Such differences can be attributed to the morphological characteristic of the powder sample, most precisely the growth of crystallites with preferential orientation [42].

Infrared spectra of samples **(1–3)** and in comparison of 1,3-H_2bdc and benzimidazole are shown in Figure S2 of Supporting Information.

In the spectra of polymers **(1–3)**, no bands in the region 1680–1730 cm^{-1} are visible what indicates the complete deprotonation of the carboxylic acid and coordination of the COO^- groups to the metal center. The difference between wavenumbers of asymmetric and symmetric stretching bands gives information about the coordination modes of carboxylate groups [43]. For **(1)** strong ν_{as} (COO^-) bands appear at 1625, 1606 and 1572 cm^{-1}, and ν_s (COO^-) band at 1398 cm^{-1} $\Delta\nu = 227$, 208 and 174 cm^{-1} indicates that carboxylates in **(1)** adopt various coordination modes, including monodentate and chelating and/or bidentate modes, what is consistent with single crystal structure analysis.

In the IR spectrum of coordination polymer **(2)** strong ν_{as} (COO^-) bands at around 1604 and 1537 cm^{-1}, and ν_s (COO^-) band at around 1407 cm^{-1} appeared. $\Delta\nu = 197$ and 130 cm^{-1} indicates that carboxylates in these polymers adopt bidentate bridging modes.

The bands at around 1477 and 1243 cm^{-1}, attributed to the vibrations of the aromatic ring and stretching vibration ν (C–N) of benzimidazole, respectively are also visible confirming the presence of benzimidazole in the structure of **(2)**. In the case of **(1)** the bands corresponding to benzimidazole cannot be clearly identified supposing that they are significantly shifted in comparison with the bands attributed to the pure benzimidazole.

For **(3)** the presence of strong ν_{as} (COO^-) and ν_s (COO^-) bands at 1575 and 1341 cm^{-1}, respectively and $\Delta\nu = 234$ cm^{-1} indicates a monodentate bridging mode of formate anions. This is consistent with the crystal structure analysis. The bands at around 3000 cm^{-1} are attributed to the vibrations of ν (N–H) for $(Me_2NH_2)^+$.

3.3. Thermal properties

The thermal properties of the obtained coordination polymers were investigated by thermogravimetric analysis (TGA) and the corresponding curves are presented in Fig. 6.

Coordination polymer **(1)** is stable up to 357 °C, at which temperature decomposition starts. The framework collapses in two steps; first mass loss up to 490 °C corresponds to the loss of coordinated benzimidazole molecules (41.72%) following the gradual loss of the carboxylate part of the framework. Presumably, at 900 °C, only the remaining ZnO is present (remaining 34.36%).

The coordination polymer **(2)** is stable up to 457 °C, at which temperature the framework starts to collapse. The two-step weight loss (44.87%) up to 630 °C corresponds to the decomposition of the benzimidazolate fragment following the gradual weight loss (25.02%) up to around 830 °C attributed to the loss of carboxylate

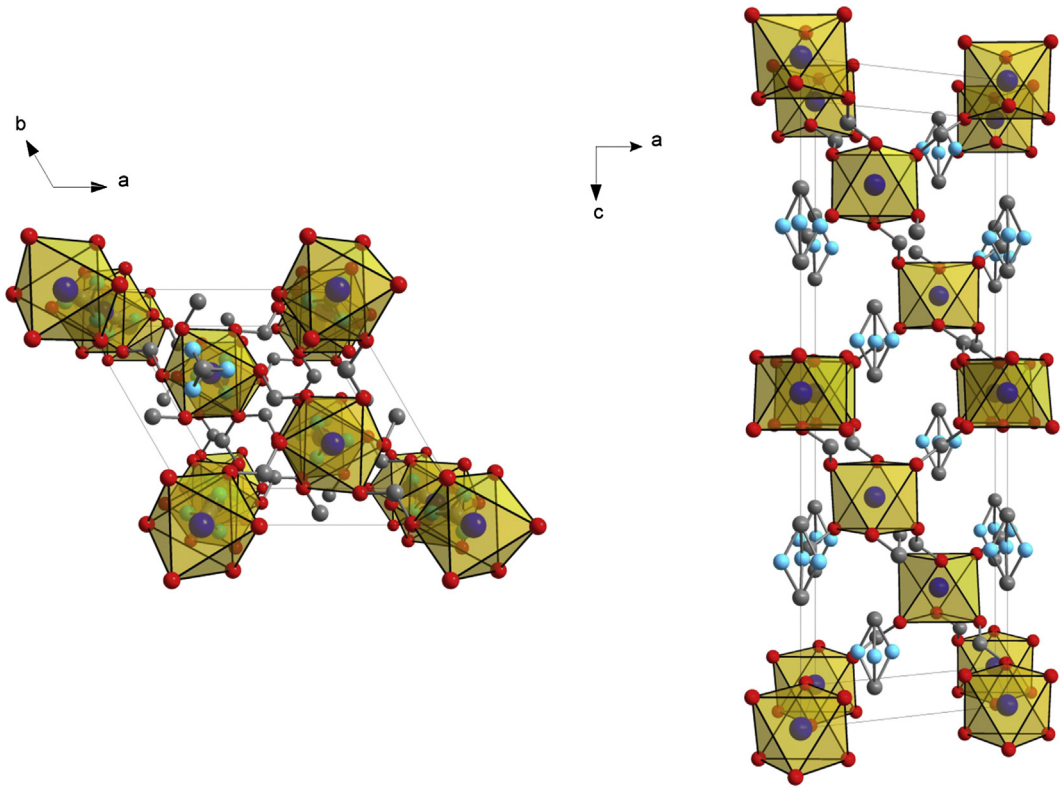

Fig. 4. Projection of (3) along c axis (on the left) and b axis showing framework channels with accommodated dimethyl ammonium cations (on the right). Zinc centers shown as yellow octahedra, hydrogen not shown. Color code: gray-carbon, red-oxygen, light blue-nitrogen, dark blue-zinc. Note: the nitrogen atom in the cation is disordered over three positions. (For interpretation of the references to colour in this figure legend, the reader is referred to the web version of this article.)

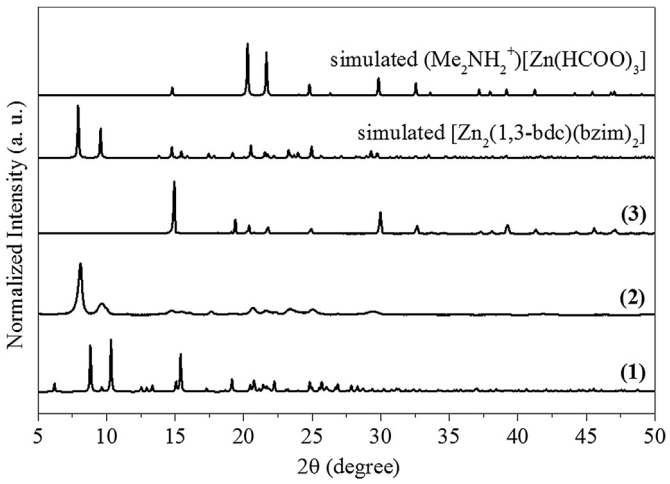

Fig. 5. PXRD patterns of obtained samples (1–3) and the simulated from single crystal data PXRD patterns of polymers $[Zn_2(1,3\text{-bdc})(bzim)_2]$ and $(Me_2NH_2^+)[Zn(HCOO)_3]$.

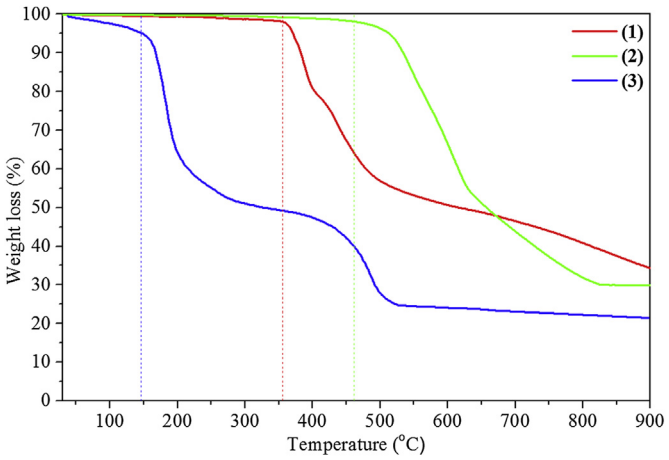

Fig. 6. TGA profiles of prepared coordination polymers (1–3).

part of the framework. Remaining 30.11% of weight is consistent with the formation of ZnO. The results indicate that the carboxylate/benzimidazolate coordination polymer **(2)** exhibit much higher thermal stability than **(1)**. Regarding the acid–base interactions, this can be explained by the stronger affinity of Zn^{2+} to nitrogen atoms present in a benzimidazole than to oxygen, leading to more stable framework in the case of **(2)**.

The least stable is the Zn-formate coordination polymer **(3)**. For **(3)**, the TGA curve shows a weight loss (4.75%) up to 146 °C, which can be attributed to the loss of approximately one molecule of adsorbed water. Comment: sample **(3)** was taken for TGA directly from the mother liquid solution; therefore the presence of a water molecule is justified. From 146 °C to 219 °C, the weight loss can be attributed to the collapse of the framework (35.7%), what according to Wang and coworkers [44] occurs via the loss of Me_2NH^+ cations located in the cages of the framework and connected to the $HCOO^-$ anions through hydrogen bonds. In order to keep the charge balance of the compound, the loss of each Me_2NH^+ cation must be followed by the loss of one $HCOO^-$ anion. This is consistent with the obtained results since the theoretical mass loss (34.5%) is close to that observed by TGA. A slight deviation in the curve slope is observed in the range from 219 to 300 °C (mass loss of 9.09%)

suggesting other not identified thermal process. Finally, the last mass loss (25.5%) from 300 to 532 °C can be assigned to the total decomposition of organic compounds forming metallic Zn and/or ZnO (remaining 24.96%).

3.4. Photophysical properties

The solid state photoluminescence properties of Zn(II) coordination polymers **(1)** and **(2)** were studied at room temperature together with the free ligands 1,3-H_2bdc and Hbzim for comparison.

The excitation and emission spectra of the free ligands 1,3-H_2bdc and benzimidazole are shown in Figs. 7 and 8, respectively. Additionally, the energy diagrams with corresponding transitions in both ligands are illustrated.

The excitation spectrum of the free 1,3-H_2bdc obtained in the range of 250–370 nm by monitoring emission at 380 nm shows a broad band with the maximum at 350 nm. The emission spectrum of 1,3-H_2bdc recorded in the range of 360–370 nm ($\lambda_{ex.}$ = 350 nm) presents a broad band centered at 380 nm corresponding to the $\pi^* \rightarrow$ n transitions, what is in agreement with the literature data [45].

In the case of free benzimidazole, the excitation spectra demonstrates four bands centered at 289, 297, 390 and 480 nm by monitoring emission at 600 nm, and only one band at 289 nm by monitoring emission at 297 nm.

The emission spectra acquired upon excitation at 289 nm when monitoring emission between 293 and 400 nm was performed without a filter of absorption, whereas the monitoring of emission in the range of 400–800 nm required the use of a filter due to the light scattering effect. The spectral profile of emission shows the most intense bands at 297 (UV region) and 757 nm (IR region) and low-intensity bands in the visible region at 600 nm (orange) and two superimposed bands with a baricentrum at around 475 nm (blue). On the spectral profile of emission obtained upon excitation at 390 and 480 nm (see Figure S6 of Supporting Information) a band at around 757 nm is not observed, indicating that this emission is dependent on the population of the S_3 state and corresponds to the $S_3 \rightarrow S_2$ transition. The second emission in the IR region of lower energy (between S_2 and S_1) is not visible in the emission spectrum due to the spectral range limitation (until 800 nm).

The energy diagram constructed on the basis of excitation and emission spectra shows the radiative and internal conversion (IC) processes. The process of deactivation of the excited state S_3 is proceeding in a cascade of internal conversions. Firstly, the excited state S_3 is populated upon excitation at 289 nm, then two processes are observed: (i) emission due to the $S_3 \rightarrow S_0$ (UV range) and $S_3 \rightarrow S_2$ (NIR range) transitions, and (ii) internal conversion from S_3 to S_2 state. Subsequently, the second excited state decays radiatively to fundamental (S_0) and first excited (S_1) state with emission around 475 nm and NIR spectral range, respectively, or decays non-radiatively to excited state S_1 (IC). Finally, the excited state S_1 decays radiatively to the ground state, with emission at 600 nm.

The excitation and emission spectra of coordination polymers **(1)** and **(2)** together with their energy diagrams are shown in Fig. 9. The excitation spectrum of coordination polymer **(1)** exhibits three broad bands superimposed with the maxima at 335 nm, 365 and 440 nm ($\lambda_{em.}$ = 380 and 550 nm). PL emission spectrum of **(1)** recorded in the range of 335–880 nm ($\lambda_{ex.}$ = 335 and 365 nm) presents bands at 380 (UV region), 500 (visible region, cyan), 775 and above 850 nm (IR region).

It was not possible to attribute unequivocally the contribution of isophthalate and/or benzimidazole ligands in the photoluminescent spectra of this material due to the similarity of the emission in the ultraviolet range observed for both ligands. However, the further analysis of full spectral profile allowed us to assign the emission spectra mainly to benzimidazole ligand. The photoluminescence spectral profile of polymer **(1)** is slightly different from that corresponding to free ligands mentioned above what is a consequence of the coordination mode of benzimidazole ligand. The energy levels diagram of coordination polymer **(1)** was proposed based on the experimental data. Similarly to free benzimidazole, **(1)** exhibits emission due to the three excited energy levels. The cascade emission effect was observed, with emission from the S_3 and S_2 excited states to the ground state (S_0) (see diagram of coordination polymer **(1)** in Fig. 9). In addition, emissions due to the $S_3 \rightarrow S_2$ and $S_2 \rightarrow S_1$ transitions in the NIR spectral range were observed, whereas the emission from the excited state S_1 to ground the state S_0 was absent.

The photoluminescence profile of **(2)** differs significantly from that presented for **(1)**; nevertheless it is similar to that presented by Hbzim ligand. In the case of **(2)**, one excitation band centered at 333 nm is observed by monitoring emission at 370 and 590 nm (solid black line) and two other bands centered at 390 and 515 nm by monitoring emission at 590 nm (dashed black line). These bands are shifted compared to the free benzimidazole due to the effect of coordination.

PL emission spectrum of **(2)** presents bands at 370, 446 and 590 nm assigned to the $S_3 \rightarrow S_0$, $S_2 \rightarrow S_0$ and $S_1 \rightarrow S_0$ transitions, respectively, resulted from the successive internal conversion processes (see diagram of energy levels for **(2)**). Moreover, two

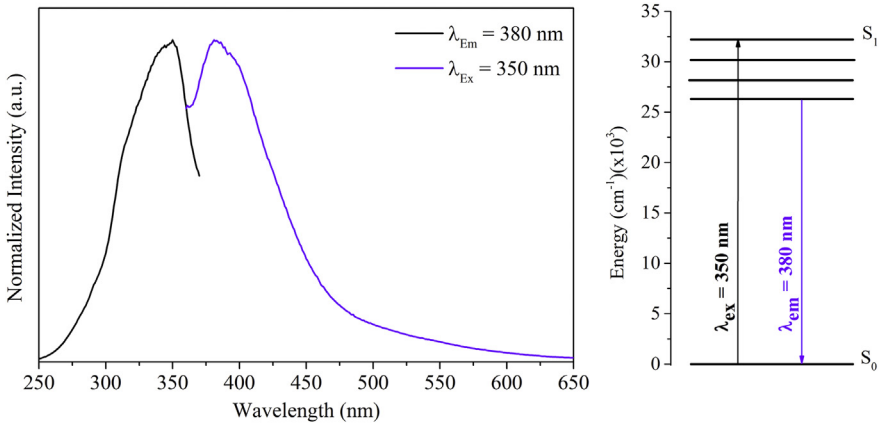

Fig. 7. Excitation and emission spectra (on the left) and energy diagram (on the right) of the free ligand 1,3-H_2bdc.

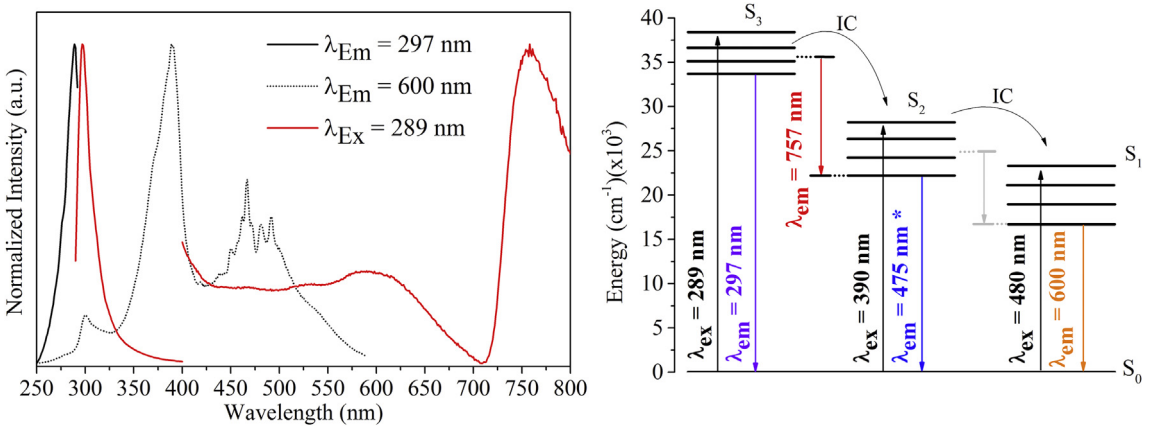

Fig. 8. Excitation and emission spectra (on the left) and energy diagram (on the right) of the free ligand benzimidazole. Transition in gray not visible in the considered spectral range.

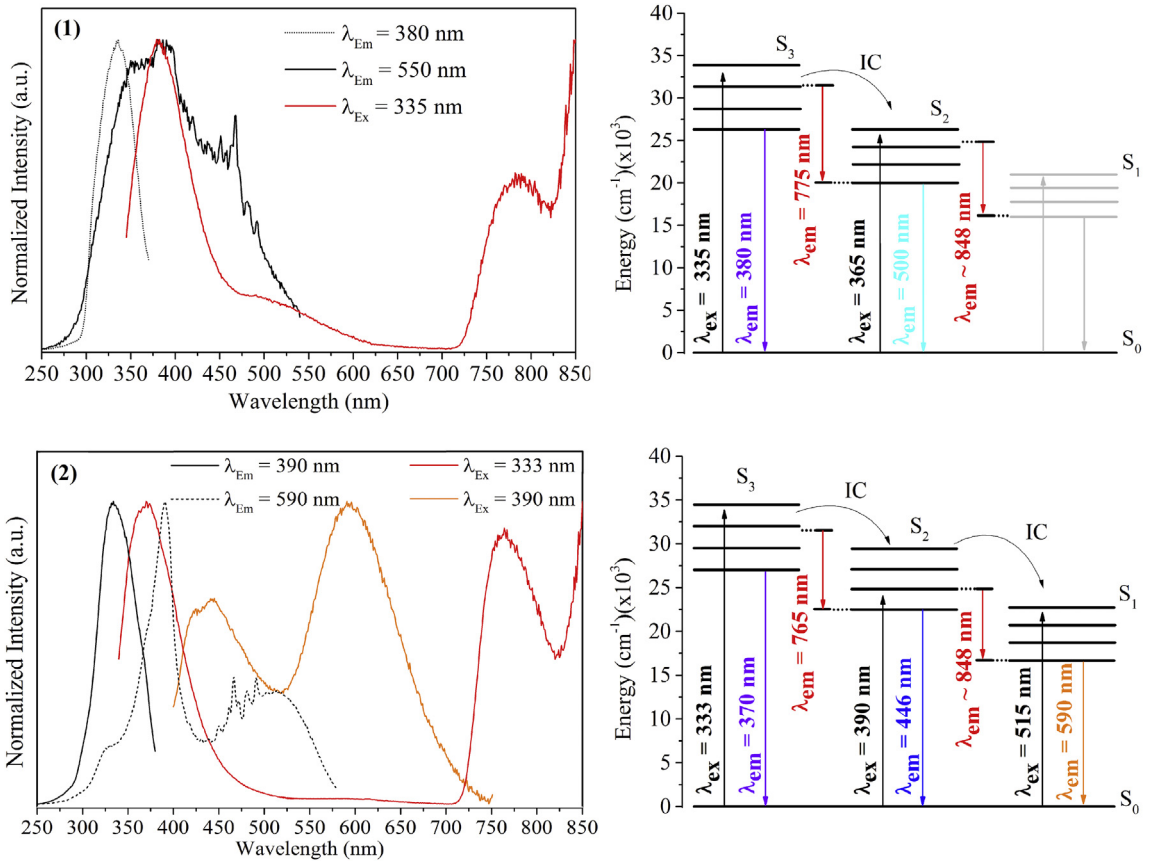

Fig. 9. Excitation and emission spectra (on the left) and energy diagram (on the right) of coordination polymer (1) and (2).

bands in the NIR spectral range at 765 and approximately at 848 nm ($\lambda_{ex.}$ = 333 nm) assigned to the $S_3 \rightarrow S_2$ and $S_2 \rightarrow S_1$ transitions, respectively were observed. When the sample was excited at 390 nm, only two bands at 446 (blue emission) and 590 nm (orange) were observed. This behavior is assigned to the population of the S_2 state. The emission due to the $S_2 \rightarrow S_1$ transition was not observed due to the experimental conditions of data acquisition (with the use of a filter).

The luminescence decay lifetimes for both linkers were measured monitoring the emission band at 380 nm, and they are comparable. Thus it is difficult to unequivocally assign this transition to one or another linker. A mixture characteristics of intraligand and ligand-to-ligand charge transition (LLCT) has already been reported for other Zn(II) complexes based on *N*-donor and *O*-donor ligands [12,46]. However, as both profiles of emission bands of **(1)** and **(2)** are similar to that obtained for the free ligand benzimidazole, therefore, the luminescence properties of these samples may be attributed mainly to the benzimidazole ligand [14].

Compared to the emission of free benzimidazole, the bands at 775 and 765 nm are red-shifted by 18 and 8 nm, for **(1)** and **(2)**, respectively. The second band found in the IR region is blue-shifted when compared to the benzimidazole spectrum and are observed

above 848 nm for both samples. Only one band at 500 nm can be observed in the visible region for **(1)** and it is red-shifted when compared to the emission spectrum of benzimidazole. For **(2)**, bands at 446 and 590 nm are blue-shifted with respect to benzimidazole. The difference in emission bands of **(1)** and **(2)** are associated with the difference in their structure topology as the fluorescence behavior is closely related to the coordination modes of the ligands and their packing in the solid state. Moreover, both polymers contain benzimidazole in different forms; protonated in the case of **(1)** and deprotonated in **(2)**. It has been reported that the protonation of the heterocyclic π-conjugated systems may cause significant shifts of emission bands also in the solid state [47].

4. Conclusions

In conclusion, it was demonstrated that the type of counter anion (acetate or nitrate) in the synthesis between Zn^{2+} salt and isophthalic acid in the presence of benzimidazole play a crucial role in the self-assembly process, yielding structurally different coordination polymers. The presence of benzimidazole, initially used as an organic base to deprotonate the organic ligand, was indispensable in these conditions. Otherwise, the Zn-formate framework was obtained, as a consequence of the hydrolysis of the solvent DMF.

Coordination polymer based on mixed isophthalate/benzimidazolate ligand **(2)** presents good thermal stability (almost up to 500 °C), much higher than found in frameworks **(1)** or **(3)** based on isophthalate/benzimidazole or formate, respectively.

The obtained coordination polymers show photoluminescence in the wide range of the spectrum, from UV to IR, and it is mainly attributed to intraligand (benzimidazole) charge transfer. Whereas **(1)** is a blue-greenish-emitter (cyan), for **(2)**, blue and orange emissions were observed. Such differences in photophysical properties are closely related to the coordination modes of the linkers as well as their packing in the solid state and the protonation effect of the benzimidazole ligand.

Acknowledgment

The authors thank Gdansk University of Technology, Universidade Federal de Pernambuco, Escola de Ciências e Tecnologia/UFRN and FACEPE.

Appendix A. Supplementary data

Supplementary data related to this article can be found at http://dx.doi.org/10.1016/j.matchemphys.2015.05.079.

References

[1] Y. Hasegawa, T. Naknishi, RSC Adv. 5 (2015) 338–353.
[2] M.L. Foo, R. Matsuda, S. Kitagawa, Chem. Mater. 26 (2014) 310–322.
[3] H. Al-Kutubi, J. Gascon, E.J.R. Sudholter, L. Rassaei, Chem. Electro. Chem. 2 (2015) 462–474.
[4] N.A. Khan, S.H. Jhung, Coord. Chem. Rev. 285 (2015) 11–23.
[5] V. Safarifard, A. Morsali, Coord. Chem. Rev. 15 (2015) 1–14.
[6] J. Xiao, Y. Wu, M. Li, B.-Y. Liu, X.-C. Huang, D. Li, Chem. Eur. J. 19 (2013) 1891–1895.
[7] N.A. Khan, Z. Hasan, S.H. Jhung, J. Hazard. Mater. 244–245 (2013) 444–456.
[8] J.-R. Li, J. Sculley, H.-C. Zhou, Chem. Rev. 112 (2012) 869–912.
[9] J. Lee, O.K. Farha, J. Roberts, K.A. Scheidt, S.T. Nguyen, J.T. Hupp, Chem. Soc. Rev. 38 (2009) 1450–1459.
[10] C.-Y. Sun, C. Qin, X.-L. Wang, Z.-M. Su, Expert Opin. Drug Deliv. 10 (2013) 89–101.
[11] Z. Su, J. Fan, T. Okamura, M.-S. Chen, S.-S. Chen, W.-Y. Sun, N. Ueyama, Cryst. Growth Des. 10 (2010) 1911–1922.
[12] Z. Xue, T. Sheng, Y. Wang, S. Hu, Y. Wen, Y. Wang, H. Li, R. Fu, X. Wu, Cryst. Eng. Comm. 17 (2015) 2004–2012.
[13] J.-D. Lin, X.-F. Long, P. Lin, S.-W. Du, Cryst. Growth Des. 10 (2010) 146–157.
[14] S.L. Xiao, L. Qin, C.H. He, X. Du, G.H. Cui, J. Inorg. Organomet. Polym. 23 (2013) 771–778.
[15] X. Zhang, L. Hou, B. Liu, L. Cui, Y.-Y. Wang, B. Wu, Cryst. Growth Des. 13 (2013) 3177–3187.
[16] M. Du, X.-J. Jiang, X.-J. Zhao, Inorg. Chem. 46 (2007) 3984–3995.
[17] X.-L. Wang, Y.-F. Bi, H.-Y. Lin, G.-C. Liu, Cryst. Growth Des. 7 (2007) 1086–1091.
[18] S.L. James, Chem. Soc. Rev. 32 (2003) 276–288.
[19] N. Stock, S. Biswas, Chem. Rev. 112 (2012) 933–969.
[20] L. Carlucci, G. Ciani, D.M. Proserpio, S. Rizzato, Cryst. Eng. Comm. 4 (2002) 121–129.
[21] Y.W. Shin, T.H. Kim, J. Seo, S.S. Lee, J. Kim, Bull. Korean Chem. Soc. 27 (2006) 1915–1918.
[22] A. Beheshti, V. Nobakht, L. Carlucci, D.M. Proserpio, C. Abrahams, J. Mol. Struct. 1037 (2013) 236–241.
[23] H.-L. Jiang, Q. Xu, Cryst. Eng. Comm. 12 (2010) 3815–3819.
[24] L. Carlucci, G. Ciani, D.M. Proserpio, S. Rizzato, Chem. Eur. J. 8 (2002) 1519–1526.
[25] H.-Y. Liu, J.-F. Ma, Y.-Y. Liu, J. Yang, Cryst. Eng. Comm. 15 (2013) 2699–2708.
[26] L. Liu, X. Li, C. Xu, G. Han, Y. Zhao, H. Hou, Y. Fan, Inorg. Chim. Acta 391 (2012) 66–71.
[27] Y.-Y. Liu, Y.-Y. Jiang, J. Yang, Y.-Y. Liu, J.-F. Ma, Cryst. Eng. Comm. 13 (2011) 6118–6129.
[28] C. Xu, Q. Guo, X. Wang, H. Hou, Y. Fan, Cryst. Growth Des. 11 (2011) 1869–1879.
[29] W. Hua, Z. LaiPing, L. HaiYan, Y. Jin, M. JianFang, Sci. China Ser. B-Chem 52 (2009) 1490–1497.
[30] H.-Y. Liu, H. Wu, J.-F. Ma, Y.-Y. Liu, B. Liu, J. Yang, Cryst. Growth Des. 10 (2010) 4795–4805.
[31] K. Yue, S. Zhao, R. Zhao, Y. Wang, Adv. Mater. Res. 399 (2012) 896–899.
[32] J. Juillard, Pure Appl. Chem. 49 (1977) 885–892.
[33] (CrysAlisPro:) Version 1.171.35.15, Agilent Technologies, Yarnton, England, 2011.
[34] L. Palatinus, G. Chapuis, J. Appl. Crystallogr. 40 (2007) 786–790.
[35] G.M. Sheldrick, Acta Crystallogr. Sect. A 64 (2008) 112–122.
[36] L.J. Farrugia, J. Appl. Crystallogr. 32 (1999) 837–838.
[37] V. Kopsky, D.B. Litvin, E (2002) 219–389.
[38] Y.-C. Cui, J.-J. Wang, B. Liu, G.-G. Gao, Q.-W. Wang, Acta Cryst. Sect. E 63 (2007) m1204–m1205.
[39] H.F. Clausen, R.D. Poulsen, A.D. Bond, M.-A.S. Chevallier, B.B. Iversen, J. Solid State Chem. 178 (2005) 3342–3351.
[40] P. Jain, N.S. Dalal, B.H. Toby, H.W. Kroto, A.K. Cheetham, J. Am. Chem. Soc. 130 (2008) 10450–10451.
[41] M. Qin, D.-H. Lee, G. Park, J. Korean Chem. Soc. 53 (2009) 73–78.
[42] M. Inoue, I. Hirasawa, J. Cryst. Growth 380 (2013) 169–175.
[43] G.B. Deacon, R.J. Phillips, Coord. Chem. Rev. 33 (1980) 227–250.
[44] X.-Y. Wang, L. Gan, S.-W. Zhang, S. Gao, Inorg. Chem. 43 (2004) 4615–4625.
[45] G.-H. Wei, J. Yang, J.-F. Ma, Y.-Y. Liu, S.-L. Li, L.-P. Zhang, Dalton Trans. (2008) 3080–3092.
[46] E.B. Coropceanu, L. Croitor, A.V. Siminel, M.S. Fonari, Polyhedron 75 (2014) 73–80.
[47] H. Detert, E. Sugiono, J. Lumin 112 (2005) 372–376.